主論文

Rheumatology, 2024, **00**, 1–12
https://doi.org/10.1093/rheumatology/keae476
Advance access publication 9 September 2024
Original Article

British Society for Rheumatology RHEUMATOLOGY OXFORD

Basic science

Association of gut commensal translocation with autoantibody production in systemic lupus erythematosus

Masao Katsushima[1,2], Yoichi Nakayama [1], Tsuneyasu Yoshida[1], Yuri Nishida[1], Mirei Shirakashi [1], Ran Nakashima [1], Hajime Yoshifuji [1], Shinji Ito[3], Junko Satoh[3], Masaki Yamamoto[4], Ryu Watanabe[2], Takashi Emori[5], Tomonori Kamiya[6], Yuko Nitahara[7], Yu Nakagama[7], Naoko Ohtani [6], Yasutoshi Kido [7], Akio Morinobu[1], Motomu Hashimoto [2,*]

[1]Department of Rheumatology and Clinical Immunology, Graduate School of Medicine, Kyoto University, Kyoto, Japan
[2]Department of Clinical Immunology, Graduate School of Medicine, Osaka Metropolitan University, Osaka, Japan
[3]Medical Research Support Center, Graduate School of Medicine, Kyoto University, Kyoto, Japan
[4]Department of Clinical Laboratory Medicine, Graduate School of Medicine, Kyoto University, Kyoto, Japan
[5]Alliance Laboratory for Advanced Medical Research, Graduate School of Medicine, Kyoto University, Kyoto, Japan
[6]Department of Pathophysiology, Graduate School of Medicine, Osaka Metropolitan University, Osaka, Japan
[7]Department of Virology and Parasitology, Graduate School of Medicine, Osaka Metropolitan University, Osaka, Japan

*Correspondence to: Motomu Hashimoto, Department of Clinical Immunology, Graduate School of Medicine, Osaka Metropolitan University, 1-4-3-13F, Asahi-cho, Abeno-ku, Osaka-shi, Osaka 545-8585, Japan. E-mail: motomu.hashimoto@omu.ac.jp

Abstract

Objective: Bacterial translocation across the gut barrier has been implicated in the pathogenesis of SLE, though the underlying mechanisms remain unclear. This study aimed to investigate the role of translocated bacteria in the context of molecular mimicry by utilizing lupus model mice and blood samples from untreated SLE patients.

Methods: Bacterial translocation was evaluated using nonselective cultured mesenteric lymph nodes (MLNs) from B6SKG mice, a lupus model characterized by impaired TCR signalling and gut dysbiosis. The relationships of detected pathobionts with autoantibody production were examined using *in vivo* experiments, ELISA, immunoblotting and epitope mapping.

Results: Culture-based bacterial profiling in MLNs demonstrated that *Lactobacillus murinus* was enriched in B6SKG mice with elevated anti-dsDNA IgG levels. Subcutaneous injection of heat-killed *L. murinus* induced anti-dsDNA IgG production without altering T- or B-cell subset composition. Immunoblotting and mass spectrometry analysis identified a peptide ATP-binding cassette (ABC) transporter as a molecular mimicry antigen, with its cross-reactivity in lupus mice confirmed by serological assays and *in vivo* immunization. The *L. murinus* ABC transporter exhibited surface epitopes that were cross-reactive with sera from lupus mice and patients. The ABC transporter from *R. gnavus*, known for its pathogenic role in lupus patients, had a similar epitope sequence to that of the *L. murinus* ABC transporter and reacted with lupus sera.

Conclusion: ABC transporters from gut bacteria can serve as cross-reactive antigens that may promote anti-dsDNA antibody production in genetically susceptible mice. These findings underscore the role of commensal-derived molecular mimicry and bacterial translocation in lupus pathogenesis.

Keywords: microbiome, systemic lupus erythematosus, molecular mimicry, bacterial translocation, ABC transporter, anti-dsDNA antibody.

Rheumatology key messages

- Gut commensal translocation to mesenteric lymph nodes contributes to anti-dsDNA antibody production in lupus mice.
- Bacterial ABC transporters can serve as molecular mimicry antigens for lupus autoantibodies.
- Common epitopes between lupus mice and patients imply potentially therapeutic targets against autoimmunity.

Introduction

SLE is characterized by production of pathogenic autoantibodies and subsequent antibody-mediated injuries [1, 2]. Anti-dsDNA antibodies react with self-antigens and trigger formation of immune complexes, thereby leading to systemic organ damage [3]. Previous studies have suggested the pathogenic potential of polyreactive autoantibodies [4–6], which can recognize both self-antigens and foreign antigens via molecular mimicry [7, 8]. SLE is also well known for its heterogeneous disease severity, which is attributed to a complex interplay between genetic and environmental factors including gut microbiota [9], though the underlying mechanisms remain elusive.

Gut dysbiosis is a significant environmental factor implicated in the pathogenesis of SLE [10], and interactions of

Received: 26 March 2024. **Accepted:** 10 August 2024

altered gut microbiota with autoreactive T cells on the intestinal mucosal layer have been shown [11]. Patients with SLE have abundant *Ruminococcus gnavus* in the gut, while the presence of anti–*R. gnavus* antibodies is significantly correlated with active nephritis [12]. Previous studies have also detected gut bacteria harbouring an Ro60 orthologue in humans [13]. Monocolonization of this pathobiont produces anti-Ro60 autoantibodies in lupus mice, while serum samples obtained from patients with SLE show cross-reactivity to the commensal Ro60 orthologue.

Bacterial translocation across the gut barrier has been speculated to be a causative factor in autoimmune diseases [14–16]. *Ruminococcus gnavus* isolated from patients with SLE was reported to increase intestinal permeability in colonized mice, resulting in its translocation to mesenteric lymph nodes (MLNs) and triggering of anti-dsDNA antibody production [17]. *Enterococcus gallinarum* DNA has been detected in liver biopsy samples of patients with SLE, while in C57BL/6 mice, monocolonization of this pathobiont resulted in its translocation to the liver and MLNs, which triggered autoantibody production [15]. Similar findings in Toll-like receptor 7 (TLR7)-transgenic C57BL/6 mice showed *Lactobacillus reuteri* translocated to MLNs, which then aggravated lupus nephritis in a TLR7-dependent manner [16]. Because of the presence of autoantigen orthologues in certain gut commensals [10, 13], bacterial translocation may directly trigger autoantibody production through molecular mimicry. Nevertheless, the specific mechanisms behind these findings remain largely unknown.

TCR signalling molecule polymorphisms are frequently noted in the genetic background of patients with SLE [18]. SKG/Jcl mice exhibit defective TCR signalling because of a point mutation in the ζ-chain-associated protein 70 (Zap70) [19], while those with a C57BL/6 background strain (i.e. B6SKG mice) develop lupus [20]. Reduced TCR signalling enables autoreactive T cells to escape thymic negative selection [21, 22], while it impairs the dynamics of microbiota-reactive T cells, leading to dysbiosis [23]. This study aimed to determine whether specific gut commensals can translocate to MLNs, and explored their contribution to SLE pathogenesis using B6SKG mice and human samples.

Methods

Animals

Mice were purchased from Japan CLEA (Tokyo, Japan) and maintained under specific pathogen-free conditions. C57BL/6 Zap70skg/skg (B6SKG) mice were created by backcrossing SKG/Jcl with C57BL/6 wild-type (WT) mice for eight generations [19, 20]. Mice 8–12 weeks old were used in this study, unless otherwise noted. Before performing experimental intervention, age- and gender-matched littermates from various parental cages were randomly mixed and assigned to each treatment group.

Human participants and sample collection

Healthy controls ($n = 6$) and untreated SLE patients ($n = 8$) were recruited from Kyoto University Hospital (Kyoto, Japan). SLE was diagnosed based on the ACR and EULAR classification criteria [24]. The clinical characteristics of the patients are listed in Supplementary Table S1, available at *Rheumatology* online. Serum samples were collected and stored at –80°C until use.

Bacterial translocation in mice

MLNs were aseptically collected, then homogenized and precultured in semisolid Gifu Anaerobic Medium (GAM, Shimadzu Diagnostics Corporation, Tokyo, Japan) for up to 7 days at 37°C. Medium contents were then streaked onto GAM agar plates and incubated in an anaerobic box for 24 h. Bacterial DNA was extracted from the cultured colonies, then amplified using a bacterial 16S rDNA PCR Kit (TaKaRa Bio, Shiga, Japan) and MiniAmp Thermal Cycler (Thermo Fisher Scientific, MA, USA). Sanger sequencing was conducted using a BigDye™ Terminator v3.1 Cycle Sequencing Kit and Applied Biosystems™ 3500xL Genetic Analyzer (Thermo Fisher Scientific).

Injection of heat-killed *Lactobacillus* species

Lactobacillus murinus and *L. reuteri* strains used in this study were isolated from MLNs of B6SKG mice. Each strain was cultured in 30 ml of 0.22-μm filtered GAM broth for 24 h at 37°C, then collected via centrifugation and washed twice with PBS. The bacterial pellets were resuspended in 1 ml of PBS and stored at –80°C. Each suspension was checked using flow cytometry and had the same number of bacteria based on order of magnitude. For heat-killed bacteria, 1 ml of bacterial suspension was thawed and heat killed at 70°C for 50 min. Subsequently, 50 μl of the suspension was streaked onto GAM agar plates and cultured for 24 h to confirm that the bacteria had been killed. For s.c. injection experiments, 100 μl of heat-killed suspensions diluted with 200 μl of PBS were used, with 300 μl of PBS used for the control.

16S rDNA amplicon sequencing

DNA extraction and 16S amplicon sequencing of mouse fecal microbiota were performed as previously described [23]. In brief, the 16S rRNA V1–V2 region was amplified using primers with adapter sequences. PCR amplicons were purified and quantified using AMPure XP beads (Beckman Coulter, CA, USA) and a KAPA library quantification kit (Nippon Genetics, Tokyo, Japan), then sequenced using a MiSeq Reagent kit v3 (600 cycles) according to the manufacturer's protocol (Illumina, CA, USA). Reads with a Phred quality score <20 and length <280 bases were filtered out. Operational taxonomic units were generated using a VSEARCH tool, with a sequence similarity threshold of 0.97. Chimeras were excluded after identification using the usearch61 program, then the taxonomic assignment was determined using the UCLUST algorithm from the Greengenes reference database (https://greengenes.secondgenome.com), with a confidence level of 0.6.

Flow cytometry

The following antibodies were purchased from BioLegend (CA, USA): anti-CD4 (RM4-5), anti-PD-1 (29F.1A12), anti-CXCR5 (L138D7), anti-B220 (RA3-6B2), anti-GL-7 (GL-7), anti-TACI (8F10), anti-CD138 (281–2), anti-IL-17 (TC11-18H10) and anti-IFN-γ (XMG1.2); from eBioscience (CA, USA): anti-CD25 (7D4), anti-FoxP3 (FJK-16s) and anti-AA4.1 (AA4.1); and from BD Biosciences (CA, USA): anti-CD95 (Jo2) and anti-Bcl-6 (K112-91); while a LIVE/DEAD™ Fixable Near IR (780) Viability Kit was purchased from Invitrogen (MA, USA). Intracellular staining was performed as previously described [20, 25]. Before cytokine staining, splenic cells were stimulated with 20 ng/ml PMA (Sigma-Aldrich, MO, USA) and 1 mM ionomycin (Sigma-

Aldrich) in the presence of GolgiStop (BD Biosciences) for 4 h. IL-17A and IFN-γ were stained after fixation and permeabilization with Cytofix/Cytoperm Solution (BD Biosciences). Before staining for the transcription factors FoxP3 and Bcl-6, splenic cells were fixed and permeabilized using the Foxp3/Transcription Factor Fixation/Permeabilization kit (eBioscience). Flow cytometric acquisition was performed using a LSRFortessa system (BD Biosciences). FlowJo software was used for analysis.

Immuno-detection of *L. murinus* antigens

Lactobacillus murinus and *L. reuteri* were lysed on ice with RIPA buffer and a protease inhibitor cocktail (Nacalai Tesque, Kyoto, Japan). Protein concentration was determined using a Bicinchoninic Acid Protein Assay Kit (Thermo Fisher Scientific, MA, USA). First, 15 μg of bacterial proteins were separated by SDS–PAGE and transferred to a PVDF membrane (Cytiva, MA, USA). The membrane was blocked, then probed overnight with mouse serum antibodies at 4°C, and incubated with Anti-Mouse IgG (H + L) and HRP Conjugate (Promega, WI, USA) for 1 h. Protein bands were detected using SuperSignal West Pico PLUS Chemiluminescent Substrate (Thermo Fisher Scientific) and digitalized with a ChemiDoc XRS Plus system (Bio-Rad, CA, USA).

Mass spectrometry of dissected protein band

Using SDS–PAGE, *L. murinus* protein lysate (15 μg) was separated with a polyacrylamide ready-made gel (e-PAGEL, ATTO, Tokyo, Japan). The gel was then stained using Coomassie brilliant blue (CBB) (EzStainAqua, ATTO) and the target band was sterilely dissected. Proteins in the band were digested and recovered using an In-gel Tryptic Digestion Kit (Thermo Fisher Scientific, MA, USA). Recovered protein digests were resuspended in 0.1% formic acid and separated using a Nano-LC Ultra 2D-plus system equipped with cHiPLC Nanoflex (Eksigent, Dublin, CA, USA) in trap-and-elute mode, with trap and analytical columns (Eksigent). The binary gradient program used for separation was as follows: A98%/B2% to A66.8%/B33.2% for 50 min, A66.8%/B33.2% to A2%/B98% for 2 min, A2%/B98% for 5 min, A2%/B98 to A98%B2% for 0.1 min and A98%/B2% for 17.9 min, with 0.1% formic acid/water and 0.1% formic acid/acetonitrile used as solvents A and B, respectively. The flow rate was 300 nl/min and the analytical column temperature was 40°C. Eluates were infused on-line to a mass spectrometer, the TripleTOF 5600+ System with NanoSpray III source and a heated interface (SCIEX, Framingham, MA, USA), and positively ionized. Data were collected using an information-dependent acquisition method and analysed using ProteinPilot software v5.0.1 (SCIEX), with the NCBI protein database for *L. murinus* (December 2020) appended with a known common contaminant database (SCIEX). Proteins were identified using Unused ProtScores, determined with the Paragon and Pro Group algorithms (SCIEX).

Generation of recombinant ABC transporter

To obtain constructs for the 6× His-tagged *L. murinus* ATP-binding cassette (ABC) transporter (WP_135942131.1), a pET expression vector was designed and transformed into BL21 Star (DE3) chemically competent *Escerichia coli* (Invitrogen, MA, USA), according to the manufacturer's instructions. After adding IPTG for a final concentration of 0.5 mM, the cells were cultured overnight at 20°C. Washed pellets were then freeze-thawed, incubated with DNase I (Roche, Basel, Switzerland), and lysed with Urea Lysis Buffer (25 mM Tris–HCl, 150 mM NaCl, 5 mM DTT, 5 M Urea, 0.5% NP 40, pH 7.8). The supernatant was purified using an His SpinTrap column (GE Healthcare, IL, USA) and stored at –30°C.

Western blotting of His-tagged ABC transporter

His-tagged ABC transporter (2.5–5 μg) was transferred to a PVDF membrane, then detected using anti-His-tag mAb-HRP-DirecT (MBL, Tokyo, Japan) for verification of the protein amount in each well. Following detection, the membrane was stripped using WB Stripping Solution (Nacalai Tesque, Kyoto, Japan), reprobed with mouse serum antibodies overnight at 4°C, and incubated with anti-Mouse IgG (H + L) and HRP Conjugate (Promega, WI, USA) for 1 h. Protein bands were detected and digitalized using ChemiDoc XRS Plus (Bio-Rad, CA, USA).

Immunization with His-tagged ABC transporter

His-tagged *L. murinus* ABC transporter (100 μg) was mixed with incomplete Freund's adjuvant (IFA, FUJIFILM, Tokyo, USA) for micelle formation. His-tagged *E. coli* LacZ with IFA was used as the control. B6SKG mice received intraperitoneal injections twice, on weeks 0 and 4. Thereafter, mouse serum samples were collected and used for anti-dsDNA antibody ELISA examinations.

ELISA

Mouse anti-dsDNA antibody titres were evaluated as previously described [23]. Correlations between anti-ABC transporter antibodies and anti-dsDNA antibodies were evaluated as described following. ELISA plates (Costar, NY, USA) were coated with 10 μg/ml of recombinant ABC transporter or 10 μg/ml of calf-thymus DNA (Thermo Fisher Scientific, MA, USA) in PBS overnight. The plates were blocked with 3% BSA in PBS, incubated with mouse or human serum antibodies for 1 h, and probed for 1 h with anti-mouse or anti-human IgG (H + L), and horseradish peroxidase (HRP) conjugate (Promega, WI, USA). Following 10 min of incubation with 3,3′,5,5′-tetramethylbenzidine, a stop solution was added, then optical density (OD) was determined at 450 nm using an iMark Microplate Absorbance Reader (Bio-Rad, CA, USA). For a neutralization assay of the anti-dsDNA antibody, a serial dilution of recombinant ABC transporter, calf-thymus DNA and *E. coli* LacZ was prepared in PBS, and added to each well of a DNA-coated plate before incubation with B6SKG mouse serum. The inhibition rate was calculated based on the percentage in OD titres determined at 450 nm.

Epitope mapping

Overlapping 15-mer peptides (shift by one or three amino acids) of the *L. murinus* or *R. gnavus* ABC transporter were spotted onto a methylcellulose membrane using a MultiPep 1 synthesizer (CEM, NC, USA) [26, 27]. After performing side chain deprotection, the membrane was blocked with Intercept Blocking Buffer (LI-COR, NE, USA), then incubated with mouse or human serum antibodies overnight at 4°C. IRDye 800CW goat anti-mouse or anti-human IgG Secondary Antibody (LI-COR) was probed for 1 h, and peptide spots were detected using an Odyssey CLx imager (LI-COR). For heatmap analysis, fluorescent intensity was normalized to the peak signal level using Odyssey software. MHCII binding

predictions were made on 20/07/2023 using the IEDB analysis resource NetMHCIIpan (v4.0) tool [28]. Whole-protein sequences of the ABC transporters from *L. murinus*, *L. reuteri* and *R. gnavus* were obtained from the NCBI database (WP_135942131.1, WP_003665824.1 and WP_268806036.1, respectively). Amino acid sequences were compared using Multalin and ESPript 3.0 software [29, 30]. The three-dimensional structures were predicted using AlphaFold2 [31], with PyMOL software used to change the epitope site colours.

Statistical analysis

All data are presented as the mean ± standard error. Group comparisons were performed using a two-tailed Student's unpaired *t*-test and comparisons of corresponding parameters using the Wilcoxon test. One-way analysis of variance followed by Tukey's multiple comparisons test were performed to compare more than two groups. GraphPad Prism (v9.4.1) and JMP Pro 14 software were used for statistical analyses. *P*-values <0.05 were considered significant.

Study approval

The study protocol was approved by the ethics committee of Kyoto University (approval number R2904) and conducted according to the Declaration of Helsinki. Written informed consent was obtained from all human participants. Mice were maintained according to the guidelines for animal care approved by Kyoto University (approval number Medkyo 16106–23104).

Results

Altered composition of translocated bacteria in MLNs from lupus mice

First, culture-based bacterial profiling in MLNs from mice was performed (Fig. 1A). We defined 'gut bacterial translocation' as the occurrence of a culture-positive result (indicating the presence of live gut commensals), in accordance with previous studies [14, 16]. We obtained culture-positive results only from MLN, but not from the liver, spleen, kidney, pancreas and whole blood (data not shown). The bacterial culture positive rates were similar between the B6SKG and WT samples (Fig. 1B). In B6SKG mice, several *Lactobacillus* species (*L. murinus*, *L. reuteri*, *L. taiwanensis*) showed more frequent detection (Fig. 1C). The bacterial composition in fecal microbiota was also compared between B6SKG and WT mice. The distribution of 16S rRNA gene amplicons belonging to major taxa did not differ at the order level (Fig. 1D), while the relative *Lactobacillus* genus amounts were similar (Fig. 1E). Then, we investigated the relationship between the levels of anti-dsDNA antibodies and bacterial species detected from MLNs. Notably, anti-dsDNA antibody titres were significantly higher in *L. murinus*-translocated B6SKG mice (Fig. 1F). These findings indicated that the bacterial composition was altered in MLNs from lupus mice and implicated the translocation of *L. murinus* in anti-dsDNA antibody production.

Autoantibody production in lupus mice injected with heat-killed *L. murinus*

Lactobacillus species are well-known gut commensals potentially protective against invasive pathogens [32, 33], thus their contributions to SLE pathogenesis were examined. Heat-killed *L. murinus* or *L. reuteri* was subcutaneously injected into B6SKG or WT mice, and the anti-dsDNA antibody titres were evaluated (Fig. 2A). *Lactobacillus murinus*–treated B6SKG mice showed significantly increased anti-dsDNA antibody titres as compared with those treated with *L. reuteri* and the controls (Fig. 2B), whereas anti-dsDNA antibody production was not seen in WT mice (Fig. 2C). These results suggest that specific commensal-derived antigens can promote autoantibody production in mice predisposed to autoimmunity.

Recent studies have reported that gut microbiota can contribute to the development of autoimmunity through two mechanisms. One mechanism is innate immune stimulation and subsequent helper T-cell differentiation, including proinflammatory Th17 [15, 34–36]. Another mechanism is molecular mimicry induced by commensal-derived antigens [13, 34, 35]. Both mechanisms can contribute to autoantibody production in lupus mice and patients [13, 15, 20, 36]. First, we investigated whether heat-killed *L. murinus* could alter the composition of certain T- and B-cell subsets, including Th cell differentiation. In both B6SKG (Fig. 2D and E) and WT mice (data not shown), flow cytometry findings of spleen cells showed no significant differences in the populations of Th1, Th17, Treg, follicular T cells (Tfh), germinal centre B or plasma cells. Then, we hypothesized that *L. murinus* may promote autoantibody production through molecular mimicry, rather than by expanding certain T- and B-cell subsets.

Identification of *L. murinus* ABC transporter as a molecular mimicry antigen

Based on speculation that *L. murinus* may harbour molecular mimicry antigens for anti-dsDNA antibodies, whether bacterial proteins can be recognized by lupus mice serum was examined. Immunoblotting of *L. murinus* lysates showed a protein band commonly detected in sera from B6SKG and MRL/lpr mice (Fig. 3A). This common protein band was sterilely dissected and analysed using mass spectrometry (Fig. 3B), with the peptide ABC transporter substrate-binding subunit protein (WP_135942131.1) identified with the highest possible level of confidence (Fig. 3C). To confirm cross-reactivity to lupus autoantibodies, a recombinant ABC transporter was generated, and subjected to CBB staining (Fig. 3D) and western blotting (Fig. 3E and F). Following verification of protein amount in each well (Fig. 3E), the membrane was subsequently stripped and reprobed using mouse serum. The results showed a strong reaction by the *L. murinus* ABC transporter to lupus mice serum that contained anti-dsDNA antibodies (Fig. 3F).

Cross-reactivity assays of *L. murinus* ABC transporter

In vitro and *in vivo* assays were conducted to confirm cross-reactivity of the *L. murinus* ABC transporter. First, serum reactivity was assessed by ELISA. As expected, the anti-ABC transporter antibody titres were significantly correlated with the anti-dsDNA antibody titres in B6SKG mice (Fig. 4A and B). Additionally, inhibition assays were conducted by adding *L. murinus* ABC transporter to anti-dsDNA ELISA plates, with the results showing partial but significant neutralization effects on binding of anti-dsDNA antibodies (Fig. 4C).

Second, B6SKG mice underwent *in vivo* immunization with *L. murinus* ABC transporter plus incomplete Freund's adjuvant (IFA). As B6SKG mice possess auto-reactive T cells due to a shift in thymic selection caused by a ZAP70 mutation, adjuvant treatment such as IFA can activate these auto-reactive T cells and elevate autoantibody levels, as previously reported [20]. Thus, we compared anti-dsDNA levels between mice

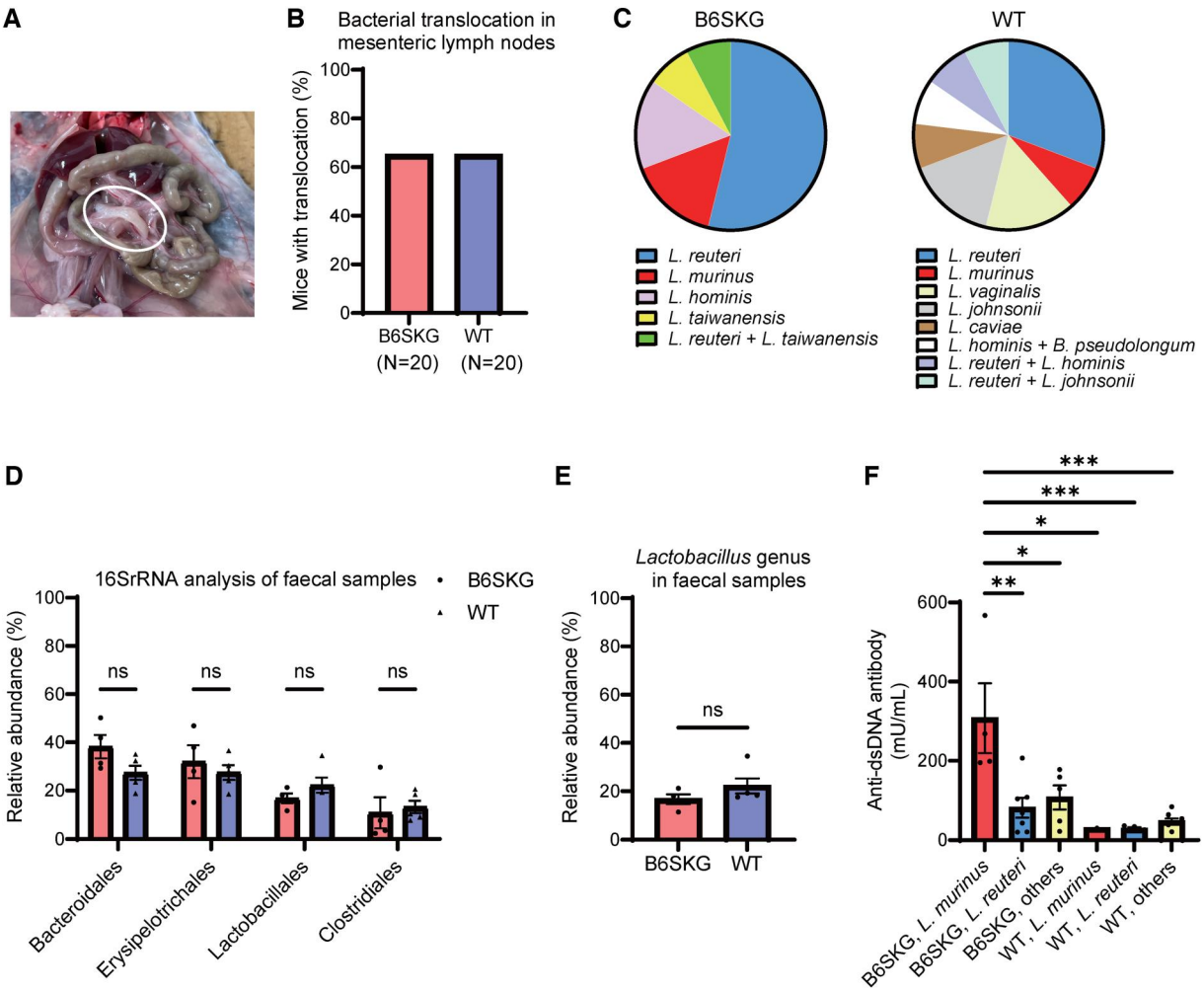

Figure 1. Altered composition of translocated gut bacteria in MLNs from lupus mice. (**A**) Sterile laparotomy of MLNs. (**B**, **C**) Total percentage of bacterial translocation in MLNs ($n = 20$) and profile of translocated species ($n = 13$). (**D**, **E**) Comparisons of fecal microbiota ($n = 4$–5) in order-level (D) and genus-level (E) taxa. (**F**) Relationship between the anti-dsDNA antibody levels and bacterial species detected from MLNs. Sixteen out of 25 B6SKG mice and 13 out of 25 WT mice showed positive results for the bacterial culture, and they were grouped based on translocated bacteria as follows: B6SKG mice with *L. murinus* ($n = 4$), *L. reuteri* ($n = 7$) and others ($n = 5$); WT mice with *L. murinus* ($n = 1$), *L. reuteri* ($n = 4$) and others ($n = 8$). Student's unpaired *t*-test was used for results shown in (D) and (E), and ANOVA for those in (F). $^{*}P < 0.05$, $^{**}P < 0.01$, $^{***}P < 0.001$, ns: not significant. MLN: mesenteric lymph node; WT: wild type

immunized with the ABC transporter + IFA and those immunized with control *E. coli* LacZ + IFA (Fig. 4D). After injection, the increase in the serum anti-dsDNA antibody levels was statistically significant in the ABC transporter + IFA group (Fig. 4E), but not in the LacZ + IFA group.

Epitope mapping of *L. murinus* ABC transporter

Lactobacillus murinus has been shown to be a gut commensal naturally found in rodents but not humans [25], thus whether the *L. murinus* ABC transporter could also be recognized by human serum was investigated. Notably, the ABC transporter showed a strong reaction to serum samples from untreated patients with SLE as compared with those from healthy controls (Fig. 5A). Furthermore, there was a significant correlation found between the anti-ABC transporter antibody and anti-dsDNA antibody titres in the participants, similar to the results of the animal experiments (Fig. 5B).

Epitope mapping was then used to determine whether the *L. murinus* ABC transporter has binding sites shared between mice and humans (Fig. 5C). B6SKG mice and patients with SLE showed similar binding patterns in heatmap analyses, with F19-25 sequences showing the highest levels of intensity (Fig. 5D).

Next, the F19-25 sequences were aligned with predicted epitopes restricted to MHC class II of the C57BL/6 strain H2-IAb or human alleles frequently observed in patients with SLE (HLA-DRB1*03:01, HLA-DRB1*15:01) (Fig. 5E). The F19-25 sequences varied between the *L. murinus* and *L. reuteri* ABC transporters, some of which were H2-IAb-restricted epitopes (observed as green and magenta). Several epitopes restricted to HLA-DRB alleles were also found in the F19-25 sequences (green, orange, magenta). Finally, the aforementioned epitopes were mapped in the predicted three-dimensional model structure (Fig. 5F) and found to be located on the protein surface near the C-terminus, suggesting that antigenic sequences are readily accessible to autoantibodies. Thus, the *L. murinus* ABC transporter is considered to be a molecular mimicry antigen with surface-exposed epitopes that are shared between lupus mice and patients.

Comparative epitope mapping of ABC transporters from *L. murinus* and human gut bacterium, *R. gnavus*

As mentioned above, *L. murinus* is reported to be absent in the human gut microbiota. Thus, we further explored

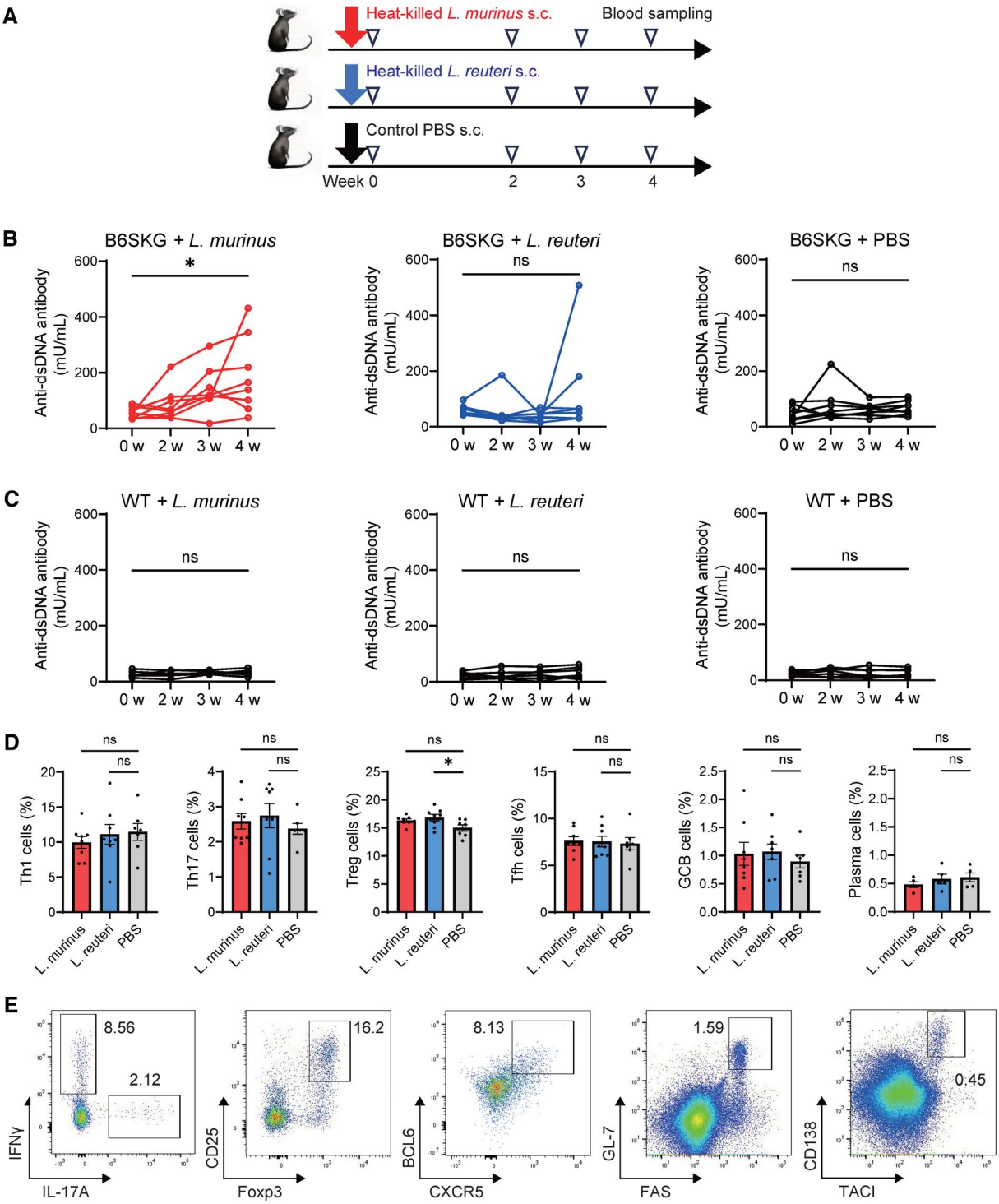

Figure 2. Autoantibody production in lupus mice injected with heat-killed *L. murinus*. (**A**) B6SKG and WT mice (anti-dsDNA antibody <100 mU/ml) subcutaneously injected with heat-killed bacteria or PBS. (**B**, **C**) Anti-dsDNA antibody levels following injection ($n = 7$–8). (**D**) Spleen cell subset proportions in B6SKG mice after 2 weeks. (**E**) T-cell subsets gated on CD4+LIVE/DEAD− (Th1: IFNγ+, Th17: IL-17A+, Treg: CD25+FoxP3+, Tfh: BCL6+CXCR5+). B-cell subsets gated on B220+ LIVE/DEAD− (germinal centre B cells: AA4.1−GL7+FAS+, plasma cells: CD138+TACI+). Wilcoxon test used for results shown in (B) and (C), and ANOVA for those in (D). *$P < 0.05$. ns: not significant. WT: wild type

whether human gut bacteria exhibit cross-reactive epitopes corresponding to the *L. murinus* ABC transporter. First, we performed a PSI-BLAST search for proteins with homology to the cross-reactive epitope of the *L. murinus* ABC transporter (YNGAGVNYNF) (Fig. 6A). We focused on *R. gnavus*, which is known to be overrepresented in the gut microbiota of lupus patients and induces anti-dsDNA antibody production when immunized in mice [12, 17]. Next,

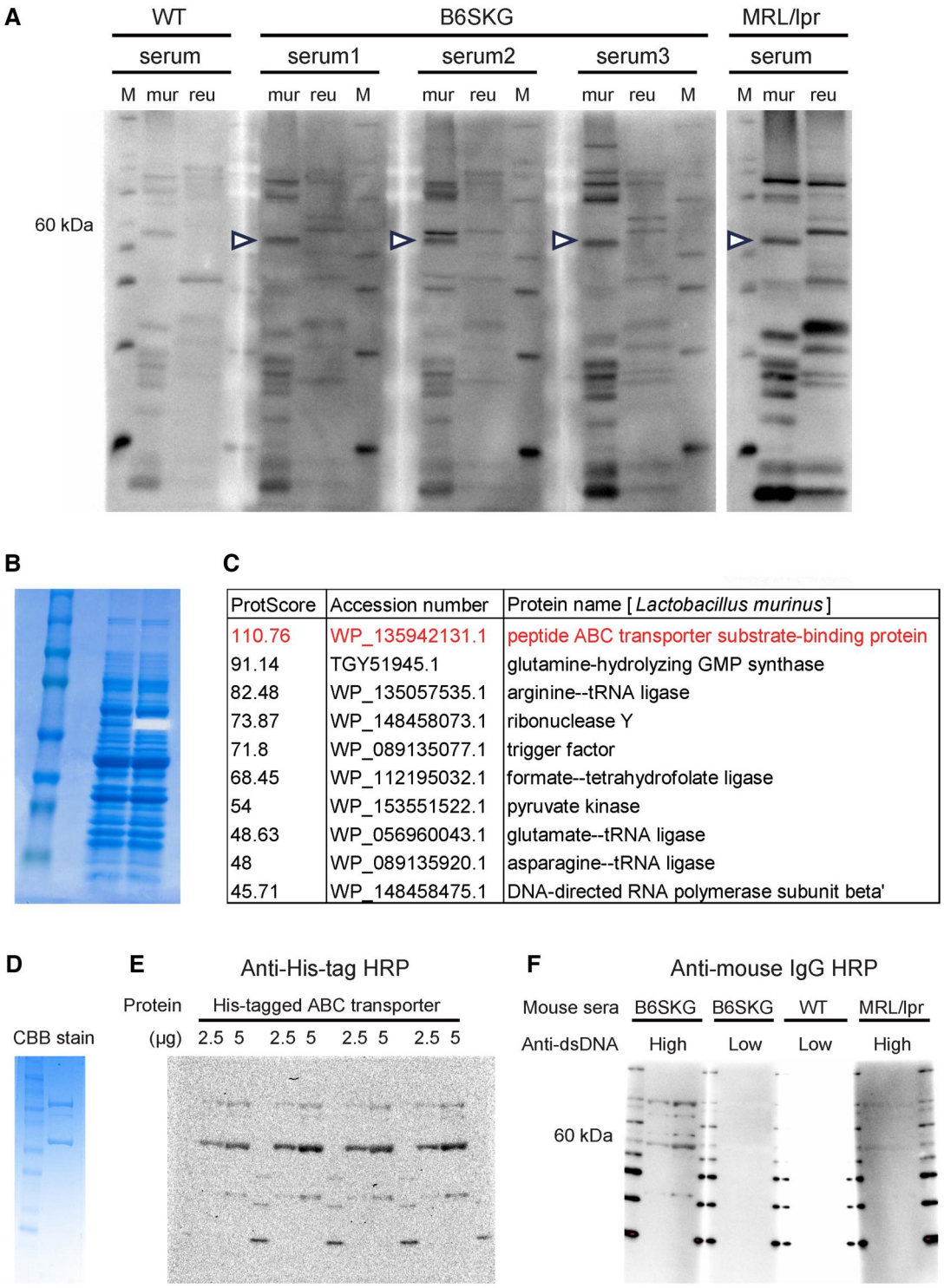

Figure 3. Identification of *L. murinus* ABC transporter as a molecular mimicry antigen. (**A**) Immunoblotting of bacterial lysates (mur = *L. murinus*; reu = *L. reuteri*; M = molecular weight marker). Triangles: protein bands commonly detected by lupus mouse sera. (**B**) *Lactobacillus murinus* lysate with CBB staining. Commonly detected band excised and analysed. (**C**) Mass spectrometry analysis. Top 10 proteins with high Unused ProtScore values are listed. (**D**–**F**) Western blotting of His-tagged ABC transporter with CBB staining. (E) Protein amount verified using anti-His-tag antibody. (F) Membrane was stripped and subsequently reprobed with mouse serum. ABC: ATP-binding cassette; CBB: Coomassie brilliant blue

we synthesized overlapping 15-mer peptides (shifted by one amino acid) of the ABC transporters in *R. gnavus* and *L. murinus*. In epitope mapping, the binding epitopes of the two ABC transporters against lupus mouse/human sera were located in nearly identical positions, differing by one amino acid residue (Fig. 6B). In the sequence alignment, the binding epitope of the *R. gnavus* ABC transporter showed sequence similarity with that of the *L. murinus* ABC transporter containing the YNGAGVNYNF sequence (Fig. 6C). Furthermore, this epitope was located on the protein surface of the *R. gnavus* ABC transporter, as shown in the predicted three-dimensional model structure. These findings suggest

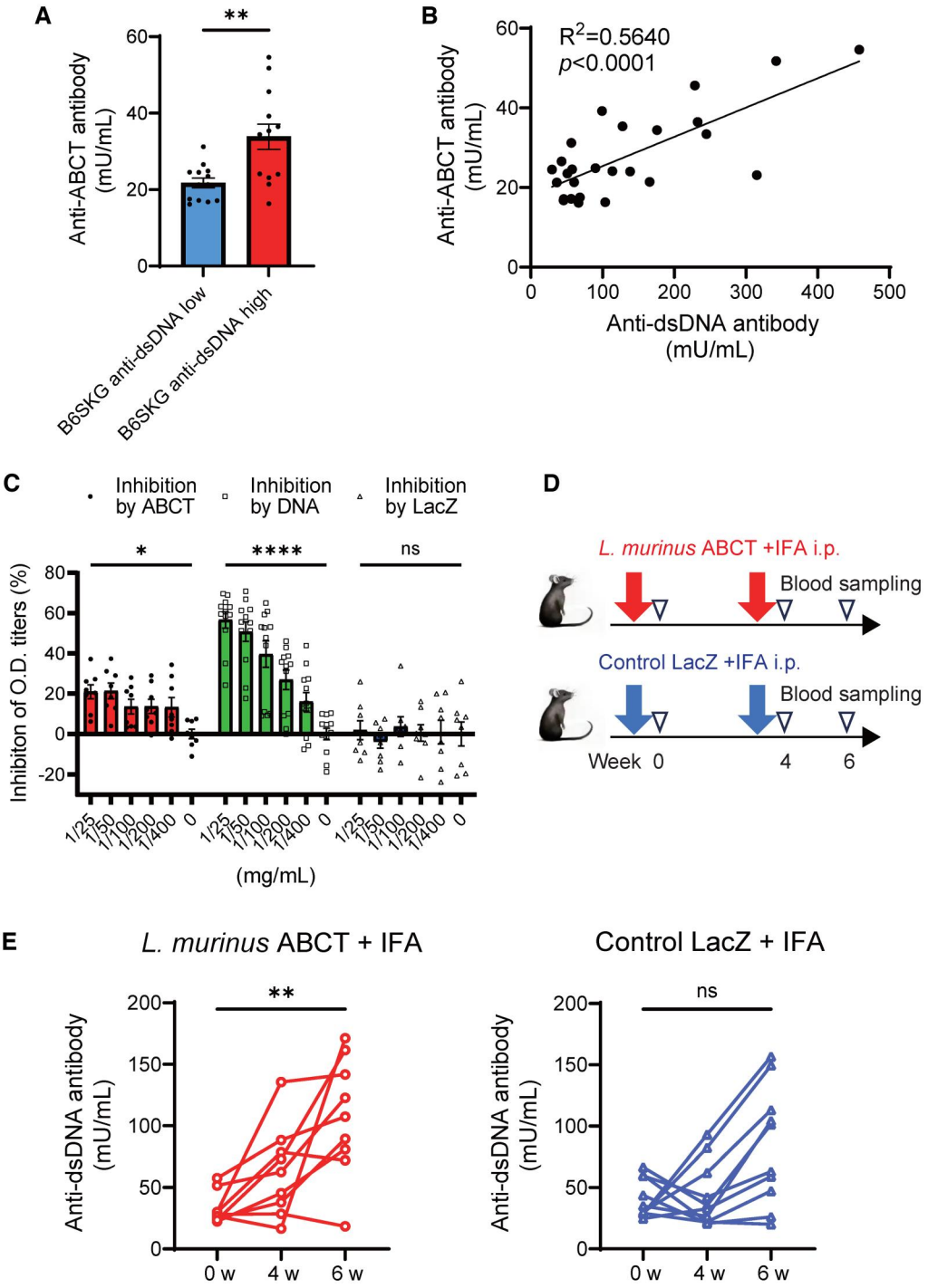

Figure 4. Cross-reactivity assays of *L. murinus* ABC transporter. (**A**, **B**) Anti-ABC transporter antibodies in B6SKG mice ($n=26$). (**C**) Neutralization assay for anti-dsDNA antibodies after adding *L. murinus* ABC transporter ($n=8$), calf-thymus DNA ($n=12$) or *E. coli* LacZ ($n=8$). (**D**) Study design of *in vivo* immunization with *L. murinus* ABC transporter. (**E**) Time-course variations of anti-dsDNA antibodies post-injection ($n=9$–10). Student's unpaired *t*-test used for results in (A), simple linear regression for those in (B), ANOVA for those in (C) and Wilcoxon test for those in (E). $^{*}P<0.05$, $^{**}P<0.01$, $^{***}P<0.0001$, ns: not significant. ABCT: ATP-binding cassette transporter; IFA: incomplete Freund's adjuvant

the presence of the cross-reactivity between gut bacteria-derived ABC transporter and lupus autoantibodies in humans.

Discussion

In this study, we found that the gut bacterium *L. murinus* translocated to the MLNs in lupus mice with high anti-dsDNA antibodies. The ABC transporter of *L. murinus* promoted anti-dsDNA antibody production when subcutaneously immunized in lupus mice and contained epitopes cross-reactive with sera from lupus mice and humans. Furthermore, this ABC transporter demonstrated similarity in epitope sequences to the ABC transporter of *R. gnavus*, known for its pathogenic potential in human lupus patients [12, 17]. These findings reinforce the hypothesis that molecular mimicry of translocated gut bacterial antigens may play a role in the production of autoantibodies in lupus.

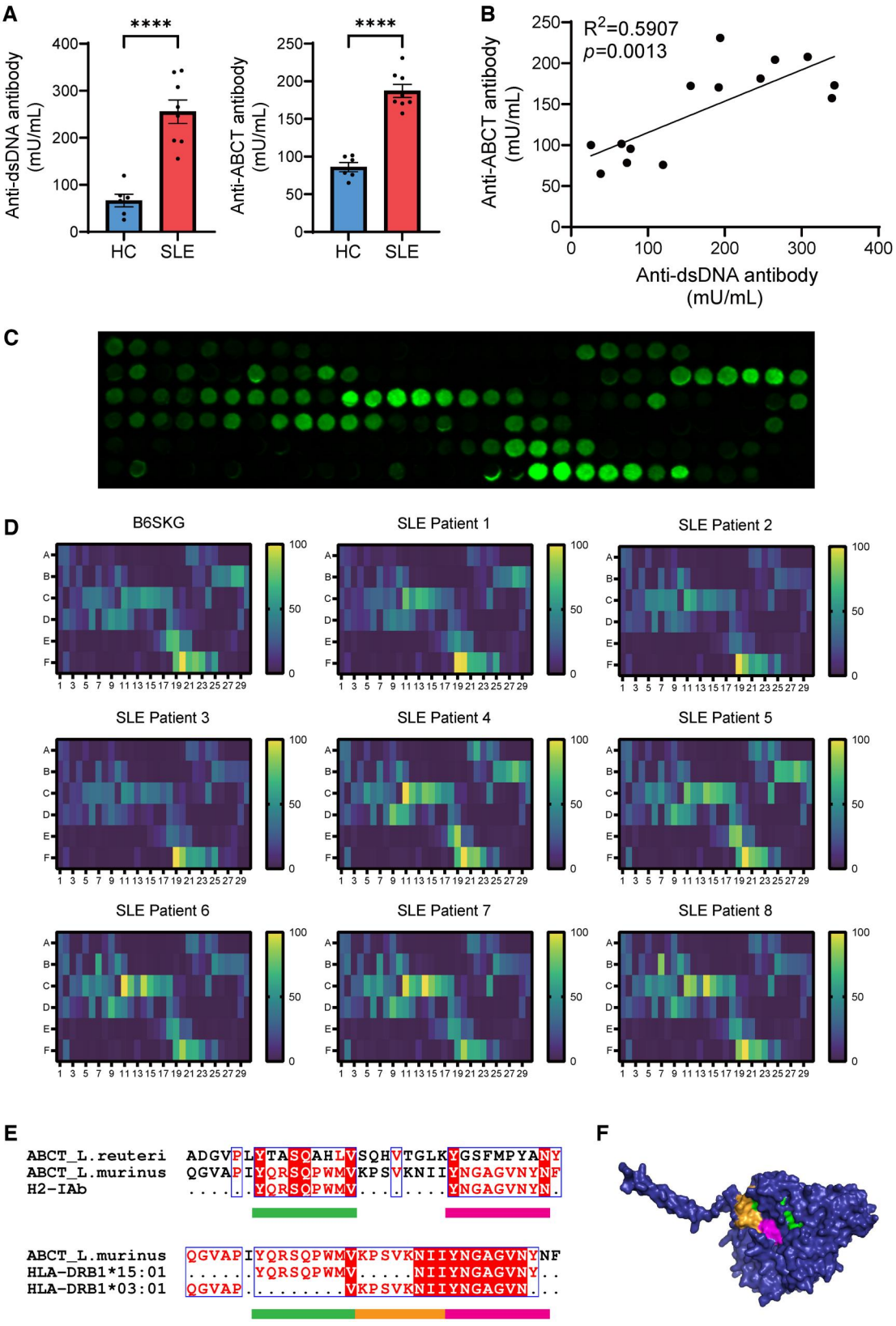

Figure 5. Cross-reactive epitopes of *L. murinus* ABC transporter shared between lupus mice and patients. (**A**, **B**) Anti-dsDNA and anti-ABC transporter antibodies in HC ($n = 6$) and SLE patients ($n = 8$). (**C**, **D**) Epitope mapping and heatmap analysis of *L. murinus* ABC transporter. (**E**) F19-25 sequences [referenced in (D)] found to be aligned with H2-IAb-restricted (top) and HLA-DRB-restricted (bottom) epitopes. Identified epitopes highlighted in green, orange and magenta. (**F**) Identified epitopes illustrated on three-dimensional model structure. Student's unpaired *t*-test used for results in (A) and simple linear regression for those in (B). $^*P < 0.0001$. ABCT: ATP-binding cassette transporter; HC: healthy controls

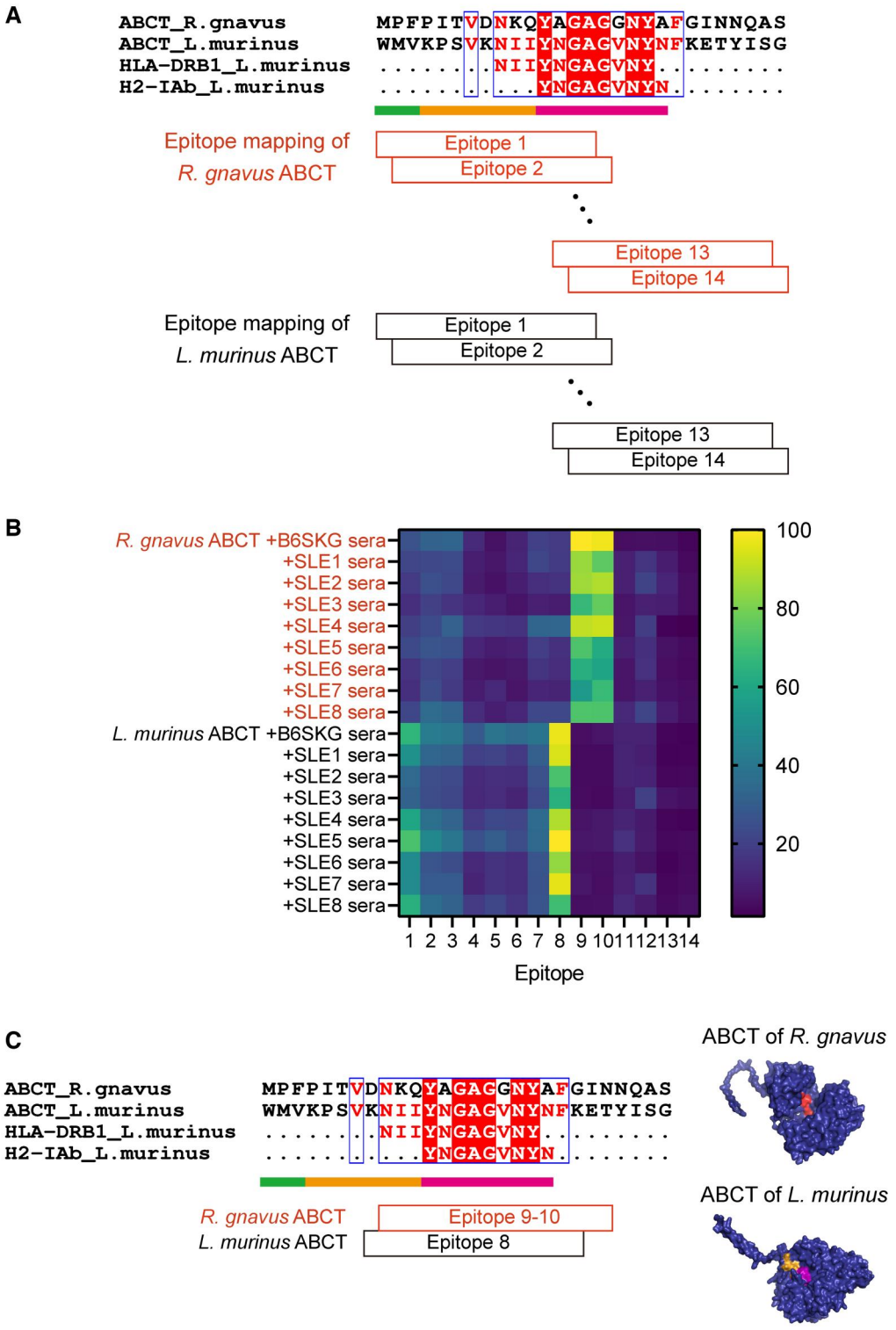

Figure 6. Comparative epitope mapping of ABC transporters from *L. murinus* and *R. gnavus*. (**A**) Sequence alignment of *R. gnavus* ABC transporter, *L. murinus* ABC transporter and MHC class II–restricted epitopes of the *L. murinus* ABC transporter. Overlapping 15-mer peptides (shift by one amino acid) of the ABC transporters were synthesized for epitope mapping. (**B**) Heatmap analysis of the epitope mapping. The synthesized 15-mer peptides were reacted with sera from B6SKG mouse and SLE patients. (**C**) Identified epitopes within the sequences of the ABC transporters. Epitope sites were also illustrated on the three-dimensional model structures. ABC: ATP-binding cassette

MLNs function as a firewall against bacterial translocation and are vital for anti-commensal immunity [37–40]. Recent studies have shown that MLNs from patients undergoing resection exhibit diverse microbiomes, with variations associated with different diseases [41]. Gut commensals can be transported to MLNs by intestinal dendritic cells [39, 42], where they activate T cells to produce commensal antigen-specific antibodies [43, 44]. Some gut commensals possess molecular mimicry antigens for autoantibodies [10, 13], including the *L. murinus* ABC transporter identified in this

study. In summary, molecular mimicry can occur following bacterial translocation to MLNs, potentially induced by bacterial cross-reactive antigens.

This study found that ABC transporters from *L. murinus* and *R. gnavus* possess similar epitope sequences that react with sera from lupus mice and patients. Interestingly, another study presented findings showing that the *C. perfringens* ABC transporter can function as a cross-reactive antigen with self-aquaporin 4 in neuromyelitis optica cases [34]. ABC transporters are ubiquitously expressed in bacteria and contain species-dependent variable regions in protein sequences. These species-dependent sequences may provide antigenic epitopes that can induce production of different autoantibodies in various autoimmune diseases.

Gut commensals have been reported to have important roles in autoimmunity through both innate and adaptive immune responses [16, 35, 45–47], as well as molecular mimicry. Based on results obtained with autoimmune animal models, molecular mimicry and Th17 differentiation are suspected to be related mechanisms [23, 35, 48]. In an experimental autoimmune encephalomyelitis model, *L. reuteri* was found to stimulate myelin oligodendrocyte glycoprotein (MOG)-specific T cells with its mimicry proteins of MOG, and another gut commensal drove Th17 differentiation [35]. In the present B6SKG model, the *L. murinus* ABC transporter promoted anti-dsDNA antibody production. In our previous study, gut dysbiosis was also found to contribute to Th17 differentiation, and thus promoted autoantibody production and lupus nephritis [23]. Bacterial translocation and activated Th17 differentiation have also been observed in patients with SLE [15, 36]. Together, these results indicate that commensal-induced molecular mimicry, Th cell differentiation and possibly other mechanisms may function together in development of autoimmune diseases.

This study has some important limitations. First, bacterial translocation evaluations were performed using nonselective culture media [49] and there may be difficult-to-culture bacteria such as obligate anaerobes. Furthermore, there could be other commensals that were undetectable because of the sensitivity limits of the present bacterial culture tests. Finally, only a single band of *L. murinus* proteins detected through immunoblotting was analysed, thus there may be mimicry proteins other than ABC transporter yet unexplored.

In conclusion, gut commensals translocated to MLNs harbour molecular mimicry epitopes that cross-react with lupus autoantibodies from mice and humans. Further exploration of these mechanisms may help elucidate novel therapeutics for systemic autoimmune diseases.

Supplementary material

Supplementary material is available at *Rheumatology* online.

Data availability

The data underlying this article made available upon reasonable request.

Funding

This work was supported by Grants-in-Aid for Scientific Research from the Ministry of Education, Culture, Sports, Science and Technology of Japan (20K08773 and 23H02945) to Motomu Hashimoto.

Disclosure statement: T.E. is an employee of Astellas Pharma, Inc. All other authors have declared that they have no conflicts of interest.

Acknowledgements

We thank Atsuko Tamamoto, Hongxin Sun and Mika Oku, of Osaka Metropolitan University, and Erika Furukawa, Tsuneo Sasai, Yuya Tabuchi, Ryosuke Hiwa, Michio Tanaka (Kyoto University), Mikako Maruya and Sidonia Fagarasan, of RIKEN Yokohama Institute, for their technical assistance. In addition, we appreciate the Medical Research Support Center of Kyoto University for performing mass spectrometry and Sanger sequencing.

References

1. Tsokos GC. Autoimmunity and organ damage in systemic lupus erythematosus. Nat Immunol 2020;21:605–14.
2. Fanouriakis A, Tziolos N, Bertsias G, Boumpas DT. Update on the diagnosis and management of systemic lupus erythematosus. Ann Rheum Dis 2021;80:14–25.
3. Wang X, Xia Y. Anti-double stranded DNA antibodies: origin, pathogenicity, and targeted therapies. Front Immunol 2019;10:1667.
4. Zhang J, Jacobi AM, Wang T *et al.* Polyreactive autoantibodies in systemic lupus erythematosus have pathogenic potential. J Autoimmun 2009;33:270–4.
5. DeGiorgio LA, Konstantinov KN, Lee SC *et al.* A subset of lupus anti-DNA antibodies cross-reacts with the NR2 glutamate receptor in systemic lupus erythematosus. Nat Med 2001;7:1189–93.
6. Mostoslavsky G, Fischel R, Yachimovich N *et al.* Lupus anti-DNA autoantibodies cross-react with a glomerular structural protein: a case for tissue injury by molecular mimicry. Eur J Immunol 2001; 31:1221–7.
7. Rojas M, Restrepo-Jimenez P, Monsalve DM *et al.* Molecular mimicry and autoimmunity. J Autoimmun 2018;95:100–23.
8. McClain MT, Heinlen LD, Dennis GJ *et al.* Early events in lupus humoral autoimmunity suggest initiation through molecular mimicry. Nat Med 2005;11:85–9.
9. Clemente JC, Manasson J, Scher JU. The role of the gut microbiome in systemic inflammatory disease. BMJ 2018;360:j5145.
10. Pan Q, Guo F, Huang Y *et al.* Gut microbiota dysbiosis in systemic lupus erythematosus: novel insights into mechanisms and promising therapeutic strategies. Front Immunol 2021;12:799788.
11. Honda K, Littman DR. The microbiota in adaptive immune homeostasis and disease. Nature 2016;535:75–84.
12. Azzouz D, Omarbekova A, Heguy A *et al.* Lupus nephritis is linked to disease-activity associated expansions and immunity to a gut commensal. Ann Rheum Dis 2019;78:947–56.
13. Greiling TM, Dehner C, Chen X *et al.* Commensal orthologs of the human autoantigen Ro60 as triggers of autoimmunity in lupus. Sci Transl Med 2018;10:eaan2306.
14. Nakamoto N, Sasaki N, Aoki R *et al.* Gut pathobionts underlie intestinal barrier dysfunction and liver T helper 17 cell immune response in primary sclerosing cholangitis. Nat Microbiol 2019; 4:492–503.
15. Manfredo Vieira S, Hiltensperger M, Kumar V *et al.* Translocation of a gut pathobiont drives autoimmunity in mice and humans. Science 2018;359:1156–61.
16. Zegarra-Ruiz DF, El Beidaq A, Iniguez AJ *et al.* A diet-sensitive commensal lactobacillus strain mediates TLR7-dependent systemic autoimmunity. Cell Host Microbe 2019;25:113–27 e6.
17. Silverman GJ, Deng J, Azzouz DF. Sex-dependent Lupus Blautia (Ruminococcus) gnavus strain induction of zonulin-mediated

intestinal permeability and autoimmunity. Front Immunol 2022; 13:897971.
18. Wang Y, Chen S, Chen J *et al.* Germline genetic patterns underlying familial rheumatoid arthritis, systemic lupus erythematosus and primary Sjogren's syndrome highlight T cell-initiated autoimmunity. Ann Rheum Dis 2020;79:268–75.
19. Sakaguchi N, Takahashi T, Hata H *et al.* Altered thymic T-cell selection due to a mutation of the ZAP-70 gene causes autoimmune arthritis in mice. Nature 2003;426:454–60.
20. Matsuo T, Hashimoto M, Sakaguchi S *et al.* Strain-specific manifestation of lupus-like systemic autoimmunity caused by Zap70 mutation. J Immunol 2019;202:3161–72.
21. Tanaka A, Maeda S, Nomura T *et al.* Construction of a T cell receptor signaling range for spontaneous development of autoimmune disease. J Exp Med 2023;220:e20220386.
22. Takeuchi Y, Hirota K, Sakaguchi S. Impaired T cell receptor signaling and development of T cell-mediated autoimmune arthritis. Immunol Rev 2020;294:164–76.
23. Shirakashi M, Maruya M, Hirota K *et al.* Effect of impaired T cell receptor signaling on the gut microbiota in a mouse model of systemic autoimmunity. Arthritis Rheumatol 2022;74:641–53.
24. Aringer M, Costenbader K, Daikh D *et al.* 2019 European League Against Rheumatism/American College of Rheumatology classification criteria for systemic lupus erythematosus. Arthritis Rheumatol 2019;71:1400–12.
25. Wilck N, Matus MG, Kearney SM *et al.* Salt-responsive gut commensal modulates T(H)17 axis and disease. Nature 2017; 551:585–9.
26. Nitahara Y, Nakagama Y, Kaku N *et al.* High-resolution linear epitope mapping of the receptor binding domain of SARS-CoV-2 spike protein in COVID-19 mRNA vaccine recipients. Microbiol Spectr 2021;9:e0096521.
27. Hilpert K, Winkler DF, Hancock RE. Peptide arrays on cellulose support: SPOT synthesis, a time and cost efficient method for synthesis of large numbers of peptides in a parallel and addressable fashion. Nat Protoc 2007;2:1333–49.
28. Reynisson B, Alvarez B, Paul S, Peters B, Nielsen M. NetMHCpan-4.1 and NetMHCIIpan-4.0: improved predictions of MHC antigen presentation by concurrent motif deconvolution and integration of MS MHC eluted ligand data. Nucleic Acids Res 2020; 48:W449–54.
29. Corpet F. Multiple sequence alignment with hierarchical clustering. Nucleic Acids Res 1988;16:10881–90.
30. Robert X, Gouet P. Deciphering key features in protein structures with the new ENDscript server. Nucleic Acids Res 2014; 42:W320–4.
31. Cramer P. AlphaFold2 and the future of structural biology. Nat Struct Mol Biol 2021;28:704–5.
32. Tang C, Kamiya T, Liu Y *et al.* Inhibition of dectin-1 signaling ameliorates colitis by inducing lactobacillus-mediated regulatory T cell expansion in the intestine. Cell Host Microbe 2015; 18:183–97.
33. Pan F, Zhang L, Li M *et al.* Predominant gut Lactobacillus murinus strain mediates anti-inflammaging effects in calorie-restricted mice. Microbiome 2018;6:54.
34. Varrin-Doyer M, Spencer CM, Schulze-Topphoff U *et al.* Aquaporin 4-specific T cells in neuromyelitis optica exhibit a Th17 bias and recognize Clostridium ABC transporter. Ann Neurol 2012;72:53–64.
35. Miyauchi E, Kim SW, Suda W *et al.* Gut microorganisms act together to exacerbate inflammation in spinal cords. Nature 2020; 585:102–6.
36. Lopez P, de Paz B, Rodriguez-Carrio J *et al.* Th17 responses and natural IgM antibodies are related to gut microbiota composition in systemic lupus erythematosus patients. Sci Rep 2016; 6:24072.
37. Macpherson AJ, Smith K. Mesenteric lymph nodes at the center of immune anatomy. J Exp Med 2006;203:497–500.
38. Wiest R, Lawson M, Geuking M. Pathological bacterial translocation in liver cirrhosis. J Hepatol 2014;60:197–209.
39. Hand TW, Dos Santos LM, Bouladoux N *et al.* Acute gastrointestinal infection induces long-lived microbiota-specific T cell responses. Science 2012;337:1553–6.
40. Belkaid Y, Bouladoux N, Hand TW. Effector and memory T cell responses to commensal bacteria. Trends Immunol 2013; 34:299–306.
41. Kiernan MG, Coffey JC, McDermott K *et al.* The human mesenteric lymph node microbiome differentiates between crohn's disease and ulcerative colitis. J Crohns Colitis 2019;13:58–66.
42. Macpherson AJ, Uhr T. Induction of protective IgA by intestinal dendritic cells carrying commensal bacteria. Science 2004;303:1662–5.
43. Slack E, Hapfelmeier S, Stecher B *et al.* Innate and adaptive immunity cooperate flexibly to maintain host-microbiota mutualism. Science 2009;325:617–20.
44. Worbs T, Bode U, Yan S *et al.* Oral tolerance originates in the intestinal immune system and relies on antigen carriage by dendritic cells. J Exp Med 2006;203:519–27.
45. Rosenkranz ME, Schulte DJ, Agle LM *et al.* TLR2 and MyD88 contribute to Lactobacillus casei extract-induced focal coronary arteritis in a mouse model of Kawasaki disease. Circulation 2005; 112:2966–73.
46. Lin IC, Suen JL, Huang SK *et al.* Dectin-1/Syk signaling is involved in Lactobacillus casei cell wall extract-induced mouse model of Kawasaki disease. Immunobiology 2013;218:201–12.
47. Mu Q, Cabana-Puig X, Mao J *et al.* Pregnancy and lactation interfere with the response of autoimmunity to modulation of gut microbiota. Microbiome 2019;7:105.
48. Maeda Y, Kurakawa T, Umemoto E *et al.* Dysbiosis contributes to arthritis development via activation of autoreactive T cells in the intestine. Arthritis Rheumatol 2016;68:2646–61.
49. Ito T, Sekizuka T, Kishi N, Yamashita A, Kuroda M. Conventional culture methods with commercially available media unveil the presence of novel culturable bacteria. Gut Microbes 2019;10:77–91.

Rheumatology, 2024, 00, 1–12
https://doi.org/10.1093/rheumatology/keae476
Original Article